Chapter 2

Instrumentations

This chapter deals with a brief description of the fundamental aspects and experimental set up of characterization techniques that we have used during our research work for studying morphological, structural, optical and electrochemical properties of synthesized composite materials.

Characterization Techniques

2.1 Tubular furnace

This tubular furnace has been used in pyrolysis purpose for preparation of the porous carbon from aquatic weed-*Eichhorniacrassipes* bio-mass under N_2 gas flow with desired temperatures variation *viz*. 600ºC, 700ºC and 800 ºC.

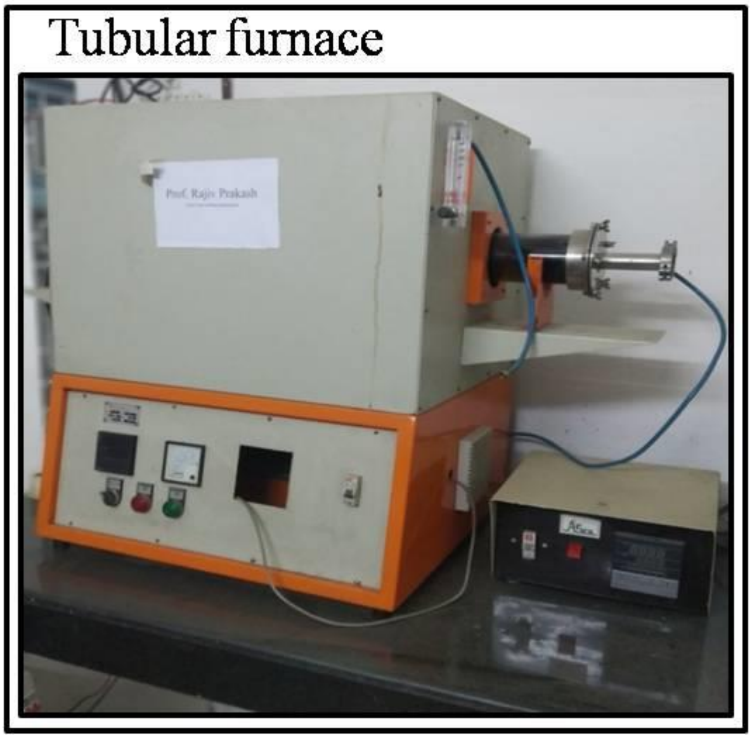

Figure 2.1 Real photograph of tubular furnace.

2.2 Thermogravimetric analysis (TGA)

Thermogravimetric analysis (TGA) is a very important and practical guided technique that helps to investigate the thermal properties or thermal stability of synthesized materials. TGA measures the amount of mass loss of material under applied temperatures in dynamic condition. The basic machinery of a typical TG also called thermo-balance are enlisted diagrammatically as in Figure 2.2. In the TG curve, the y-axis representing the mass (m) which is decreasing downwards (ordinate), and the x-axis shows the temperature (T) as increasing sequence from left to right (abscissa). In the present work, the TG analysis was conducted on Mettler Toledo (TGA/DSC 1 ATARE system, Switzerland) by using calculated quantity of samples with in the temperature from 30°C to 900°C at the heating rate of 10°C/min.

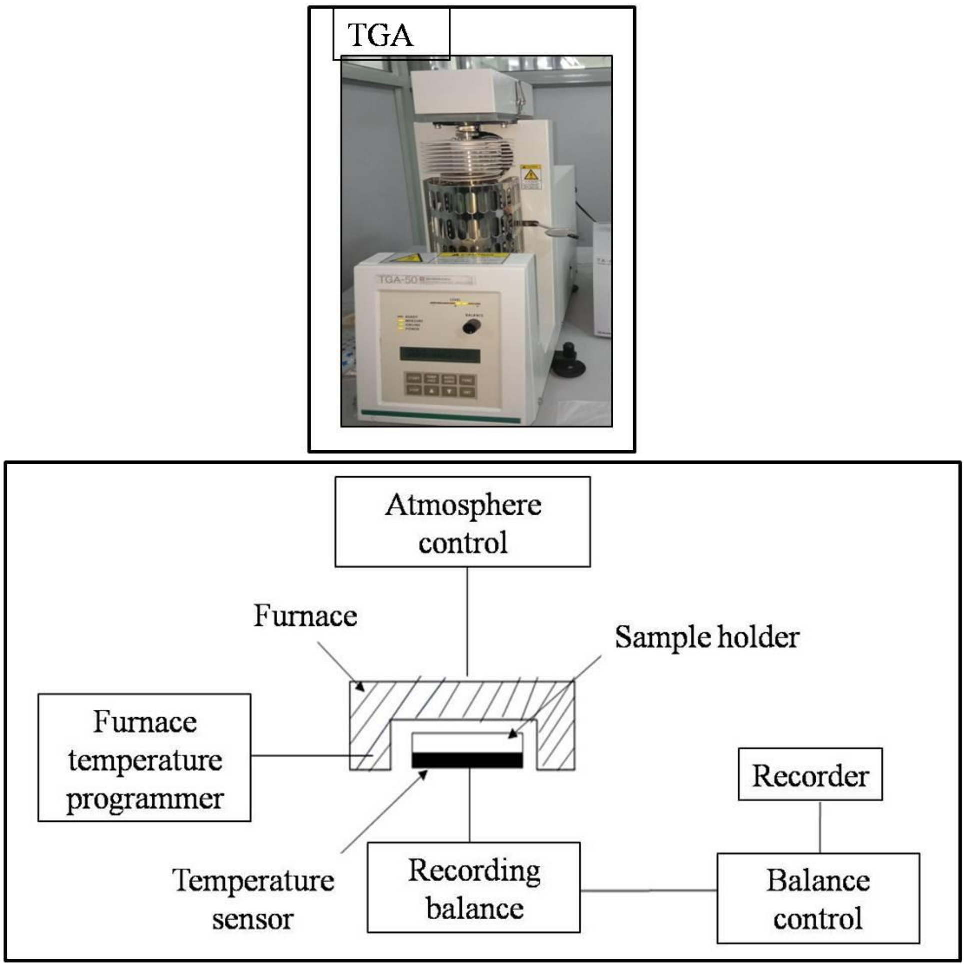

Figure 2.2 TGA instruments and its Block diagram of Thermo- balance.

2.3 Scanning Electron Microscopy (SEM)

SEM is a technique gives detail information and magnification imaging or surface topography of our desired samples. The photograph of SEM instruments and layout of components is shown in Figure 2.3. For this experiment, the sample has prepared either by the direct sprinkling of powder sample over conducting carbon tape surface or drop-casting of dispersion of samples (in highly volatile solvent) on the hard metallic aluminium stub. After this, a thin layer of gold coating is sphuttered over the sample surface, which protects the charging/ burning of samples under the high energy electron beam. This as-prepared sample stub is now placed inside the sample stage chamber of SEM instrument where an electron gun located near the sample which emits high energy electrons. The electrons beam allow to interact with the sample and produce various signals depending on the penetration depth of the electron beam [Skook et al. (2010)]. The morphological studiesof our synthesized materials in the present thesis were done on ZISS |EVO|18| research instrument with an acceleration voltage of 2 kV to 15 kV.

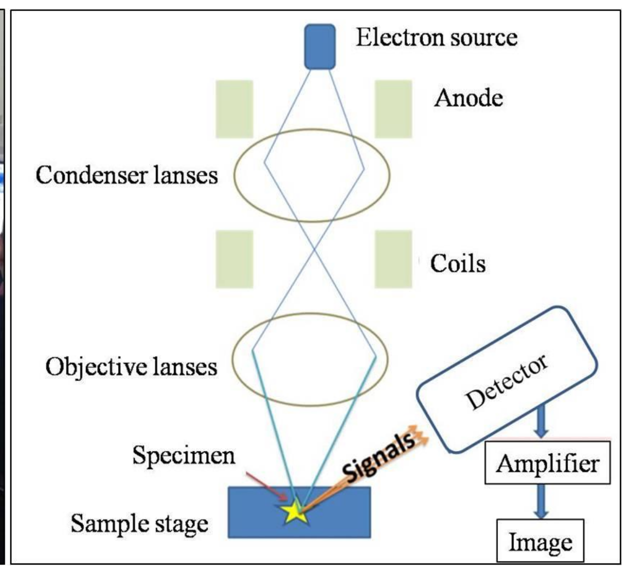

Figure 2.3 Photograph of SEM instruments and schematic layout of different components of the SEM.

2.4 Transmission Electron Microscopy (TEM)

Figure 2.4 is representing a high-resolution transmission electron microscope (HR-TEM) instrument photograph in a specification model FEI TECNAI G^2 F20-Twin, Swiss Republic at an operating voltage of 200 kV. TEM offers advance morphological imaging of nanomaterials with detailed information about crystalline structure under a selected area electron diffraction (SAED) pattern phenomenon. This instrument works like a light microscope, where glass lenses are replaced by magnetic coils, and the electron beem is used as the illuminating source [Williams et al.]. Herein, TEM experiment, samples were prepared by dispersing the synthesized materials in volatile solvent and drop-casted over carbon coated copper grid. After that this coated grid is allowed to place on sample holder.

Figure 2.4 Photograph of TEM instruments.

2.5 **Atomic force microscopy** (AFM)

AFM was used in order to study the 3D surface structure and phase contrast micrograph of nanomaterials. Surface study of porphyrin functionalized PIn and PIn (in chapter 6) was done on scanning probe microscope (SPM) (specification: NTEGRA prima, NT-MDT Service & logistic Ltd.) as shown in Figure 2.5. In this technique, surface topography is recored and based on the deflection of laser during the raster scanning of caltiliver having carbon nano tip.

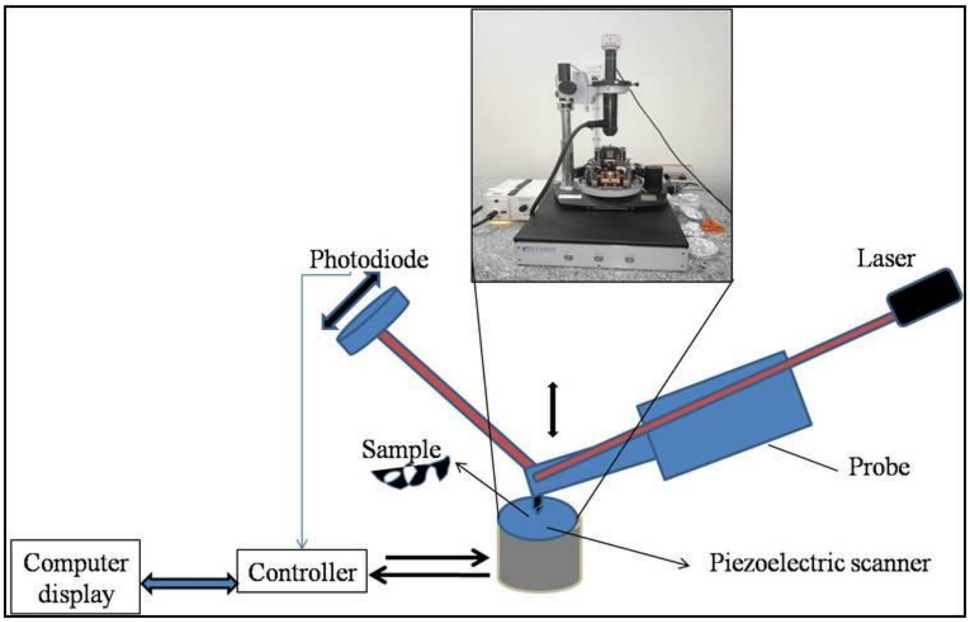

Figure 2.5 Schematic diagram of AFM.

2.6 Fourier Transform Infrared Spectroscopy (FT-IR)

FT-IR spectroscopy is very dedicated as well as familiar instruments for the synthesis research work which can detect the presence of specific functional groups as well as impurities. FT-IR instruments and schematic illustration about its different components are shown in Figure 2.6. These give a unique collection of bands corresponding to specific bonding for a molecule and resulting in a fingerprint to such moiety and their compound purity. Every molecule has its specific frequencies of internal vibrations which can interact with the infrared waves of the electromagnetic spectrum (~4000 cm^{-1} to ~400 cm^{-1}). When a sample is irradiated by infrared radiation of the electromagnetic range, that will absorb specific radiation frequencies related to the bond presented in material, and transmit some other frequencies. Therefore, this instrument is very important to the identification of structural and bonding within a substance because different functional group have different vibrations and give special infrared spectra [Banwell et al. (1994), Skook et al. (2010)] ..

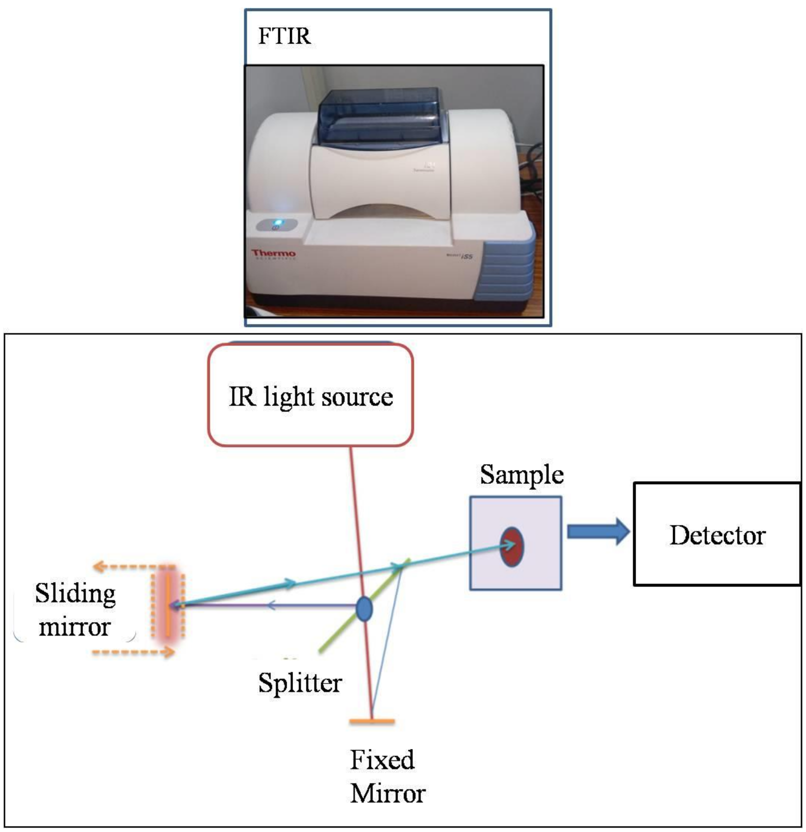

Figure 2.6 FTIR instruments and schematic illustration about its different components.

Furthermore, from the IR spectra, it is likely to conclude whether chemical functional groups are present or not in the given materials or sample. The functional groups having permanent dipole moment is only IR active. In presen thesis, the samples of chapter 3 are studied by using Attenuated total reflection (ATR) alpha Brukar eco ATR' attached with ZnSe crystal, and in chapter 4 to 6 FTIR analysis was carried out with Thermo Scientific Nicolet 6700, respectively

2.7 Raman spectroscopy

Raman spectroscopy is a highly sophisticated, non-destructive technique that leads to a specific understanding of chemical bonding in the materials. (Figure 2.7 schematic illustration of the Raman components). Change in polarizability is the basic for Raman and therefore, this technique is also known as structural fingerprint, having a set of knowledge on molecular transitions including vibrational, rotational as well as weak transition mode. Inelastic scattering of the incident monochromatic light (upon interaction with samples) which is also referred to as Raman scattering is the basic phenomenon [Banwell et al. (1994), Skook et al. (2010)]. In this thesis, all samples Raman characterization were recorded on Micro Raman Spectroscopy (renishaw, Germany) with laser light (514.5nm).

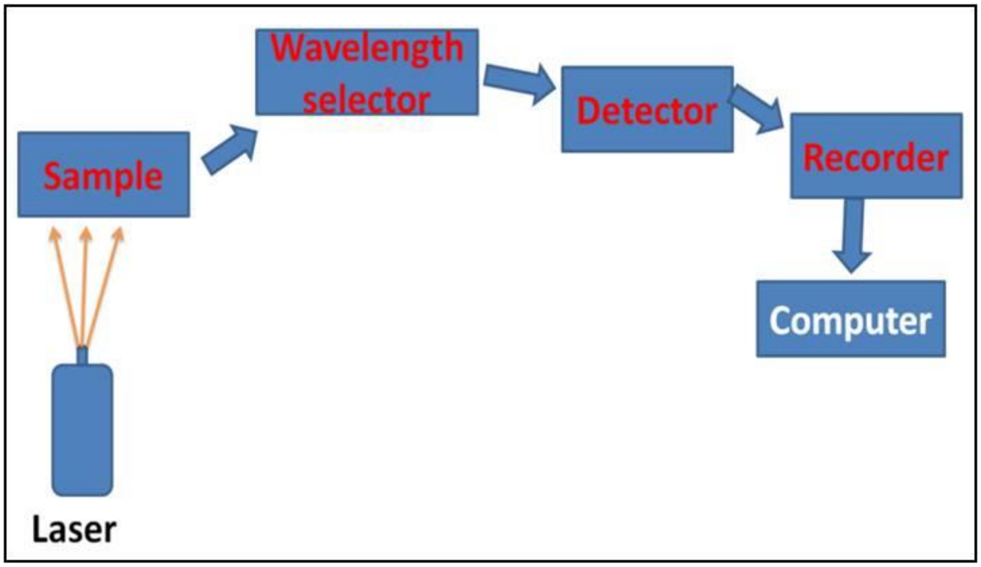

Figure 2.7 Schematic illustration of the Raman components

2.8 Nuclear Magnetic Resonance (^{1}H NMR)

Nuclear Magnetic Resonance (NMR) is used to investigate the chemical bonding in the prepared sample (as Figure 2.8 NMR instrument Bruker Advance 500 MHz). In this thesis, mode of PIn linkage and their bonding with Fe in Fe-OEP (chapter 6), the ^{1}H NMR spectra were recorded using instrument Bruker Advance 500 MHz at normal room condition. Deuterated chloroform (d_6-$CHCl_3$) and d_6-DMSO were used as a solvent. Tetramethylsilane (TMS) was used as a reference which shows a peak at 0 ppm. The NMR peak shifting (upfield and downfield) is directly related to electron density around the proton.

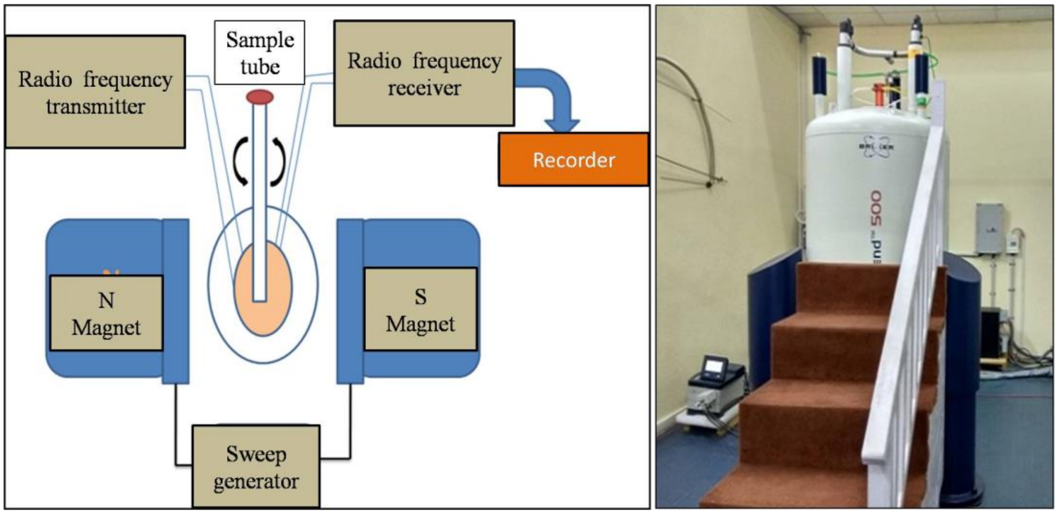

Figure 2.8 Schematic working layout and photograph of NMR.

2.9 Optical absorption spectroscopy (UV-vis absorption spectroscopy)

A UV-visible spectrophotometer is a very common and primary technique used for the encapsulation of absorbance or reflectance band of an analyte, present in the liquid phase by passing a beam of visible light or UV light (200 to 900 nm) through the sample and measuring the absorbance of the solution. The excitation of electron from ground lavel (Gs) to exited state (Es) is basic process which occer within molecule. The spectrophotometer report the plot of the wavelength of absorbed radiations as a function of the intensity of absorption (optical density or absorbance). The instrument works explained according to Lambert-Beer's law. Lambert-Beer's law can be expressed as:

$$\log_{10} I_0 / I = A = \varepsilon cl$$

where I_0 is the incident radiation intensity, I is the transmitted radiation intensity through given sample solution, A is the absorbance of optical density, ε is the molar extinction coefficient or molar absorptivity, c is the concentration (mol/L) and l is the path length of the sample (1cm) [Banwell et al. (1994)].

According to this law the fraction of incident monochromatic radiation absorbed by a homogenous medium is proportional to the number of absorbing molecules present in the given solution. In presented thesis UV Vis absorption of samples were investigated by using Biotech spectrophotometer instruments, USA (as shown in figure 2.9) by using quartz cuvette (1.0 cm path length). .

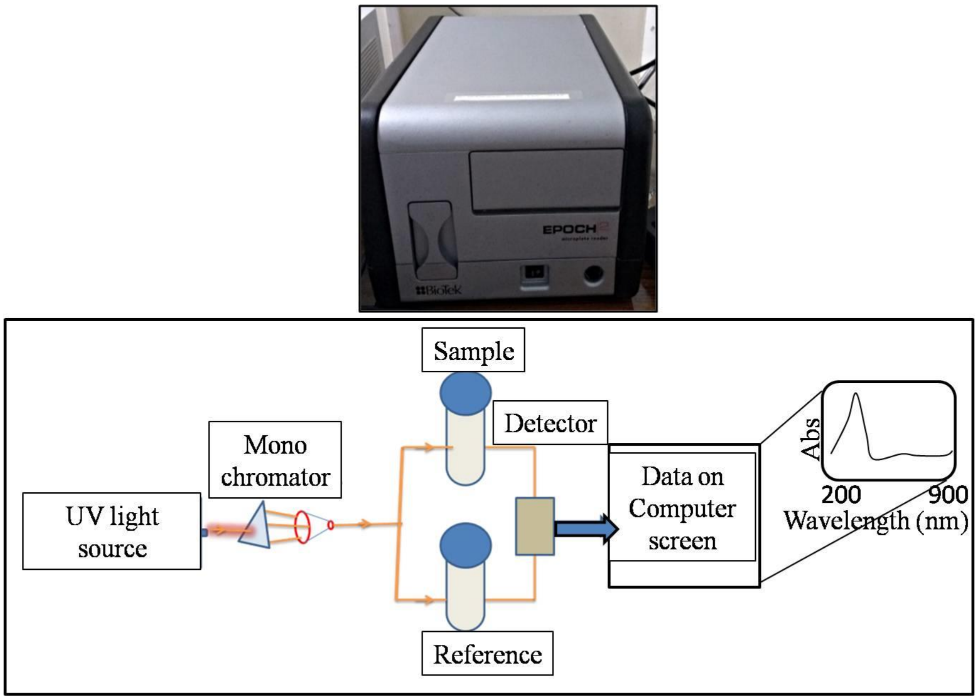

Figure 2.9 Schematic working layout of the Uv-Vis spectrophotometer and their photograph.

2.10 X-ray photoelectron spectroscopy (XPS)

This is a very sophisticated technique for investigation of the surface chemical structure and environment. In this thesis, XPS of our synthesized samples were carried out on the XPS spectrophotometer, AMICUS, U.K. The layout of the physical process implicated in XPS is represented as in Figure 2.10. In this instrument, irradiation of sample surface with X-rays beam and impact of this on the sample surface result secondry beam which is detected by the spectrophotometer and record spectrum plot in the form of intensity in count/sec *vs*. binding energy (in eV).

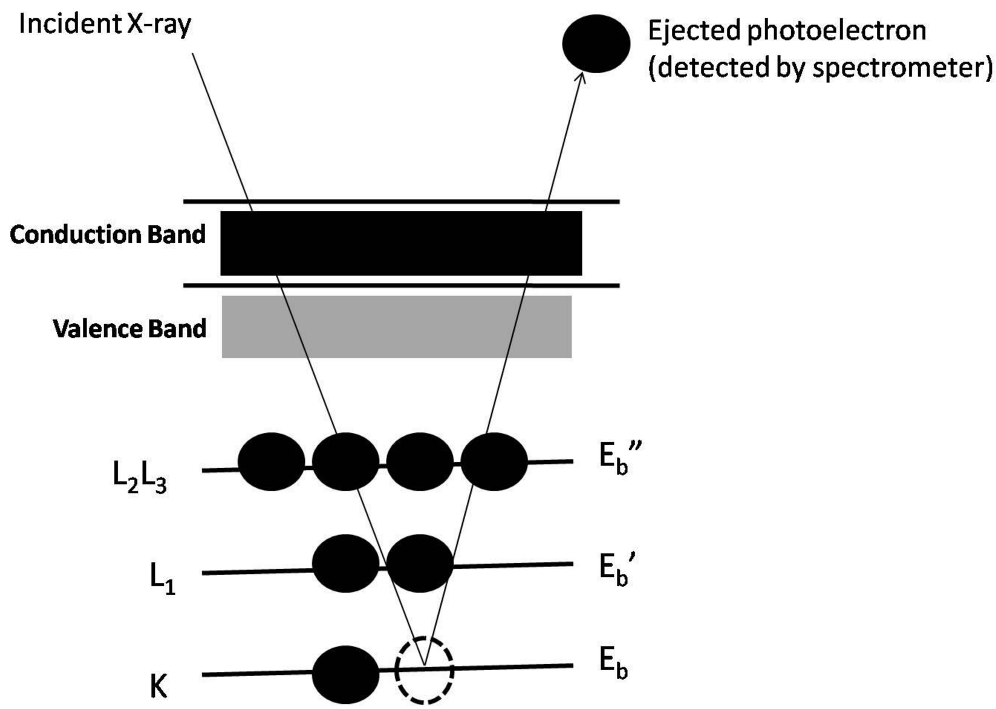

Figure 2.10 Layout of the physical process in XPS.

2.11 X-ray diffraction (XRD)

X-ray diffraction is a powerful non-destructive tool for characterizing the degree of crystallinity in the prepared nanomaterials and giving information about structures, phases, preferred crystal orientation (texture), and other structural parameters such as average grain size, crystallinity, strain, and crystal defects. In this thesis, all powder XRD diffractograms were recorded on the Rigaku MiniFlex600 Japan (figure 2.10). X-Ray diffractometer using Cu-Kα (λ 0.154nm) as a radiation source at a scan rate of 3^{o}/minute.

Figure 2.11 Photograph of XRD instrument

2.12 Electrochemistry

CH-Instruments model 7143 updated were used for electrochemical analysis of prepared materials in this thesis (Figure 2.12). This instrument composed of three electrode system.

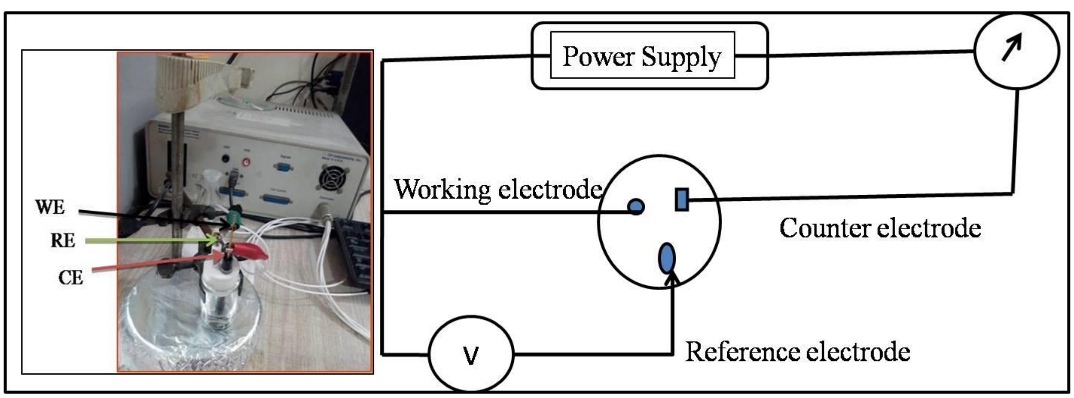

Figure 2.12 CH Instruments photograph and experimental setup.

2.12.1 Cyclic Voltammetry

Cyclic voltammetry CV) is a common and most popular screening technique to identify any electrochemical redox activity of any materials and catalysts. The experimental setup consists of three-electrode assembly viz. working, reference and counter electrode as shown in Figure 2.12. As the name suggests, the potential is cycled through a range with a constant scan rate. The potential sweeps from a start voltage to an end voltage, then back to the start, completing the cycle (Figure 2.13).

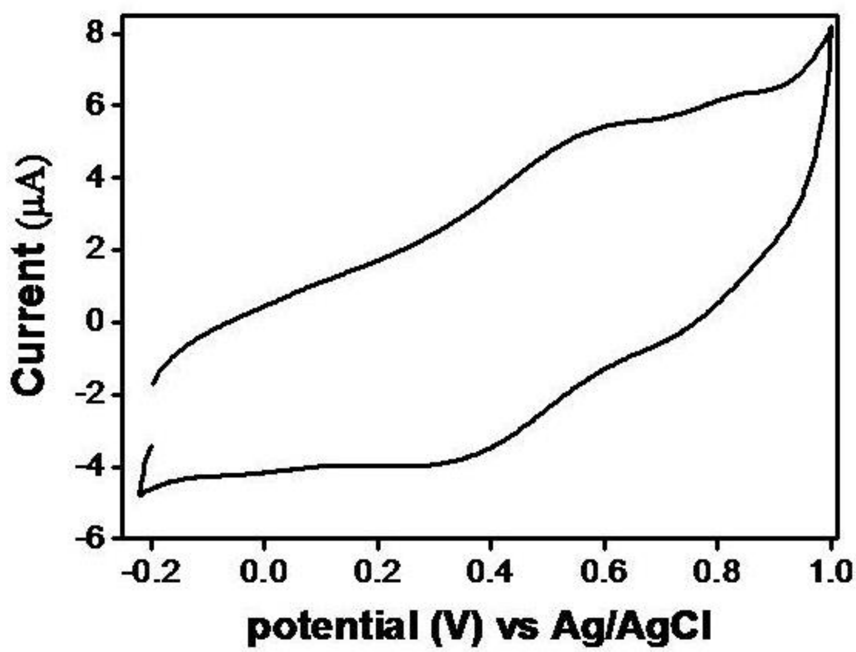

Figure 2.13 Representation of the CV curve.

2.12.2 Electrochemical impedance spectroscopy (EIS)

Electrochemical Impedance Spectroscopy (EIS) is a well known experimental tool to characterize the behavior of electrochemical systems [Bard et al.(2001)]. Therefore the results of an impedance measurement can be described in a Nyquist plot (Figure 2.14) which plots Z_{real} and Z_{img} [Lisdat et al. (2008)]. There are numerous parameters accountable for charge transfer through the electrode material-electrolytes solution interface viz. solution resistance (Rs), capacitance, charge transfer resistance(Rct), diffusion impedance, or mass transfer [Chulkinet al. (2018)]. The Nyquist plot consists of two regions: the first one is nearly at low frequency showing a straight line, and another a semi-circle (on Z'-axis) like shape appeared at high frequency. The faradaic components (appeared at high-frequency region) arise due to the charge transfer resistance, R_{ct} (redox reaction) along with the uncompensated solution resistance, R_s. Solution resistance (Rs) which is always present for all system, afforded by the ion concentration and the cell geometry.

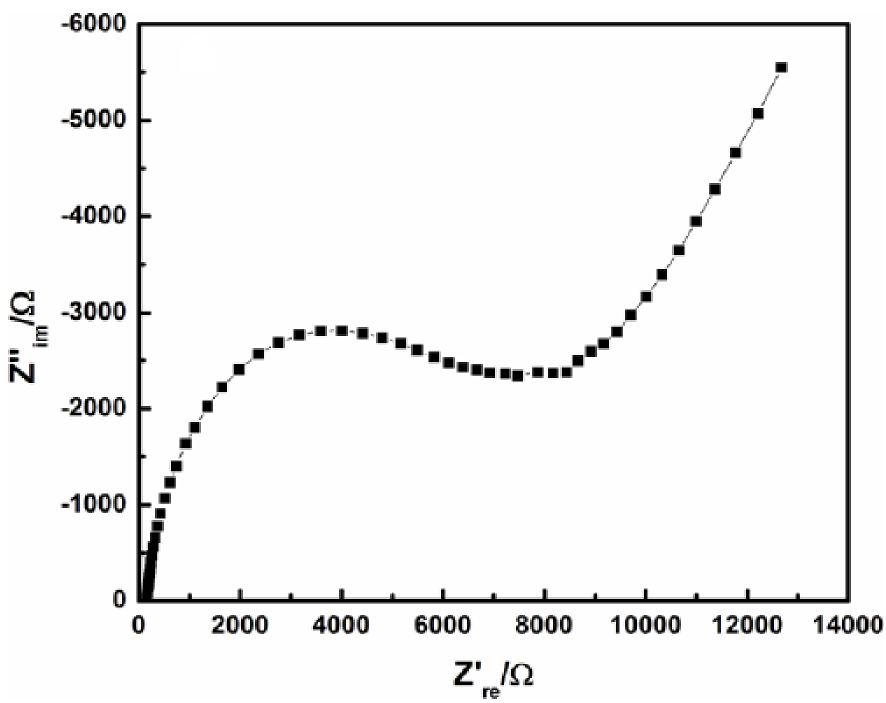

Figure 2.14 Representation of the Nyquist plot.

However, straight-line at lower frequency region showing a mass transport or change of the reactant and product also determine the speed of electron transfer. Such mass transport bestowal different type of impedance, which is known as Warburg impedance (W) (Figure 2.14) [Chang et al. (2010)].

2.12.3 Galvanostatic Charge-discharge technique

The galvanostatic charge-discharge (GCD) is a trustworthy and widely used techniques in the field of supercapacitor for the reason that it can be extended from a laboratory scale to an real practice. In this, the current is controlled and the voltage is measured. GCD is also called as chronopotentiometry and gives information about various parameters such as capacitance, resistance, and cyclability.

The specific capacitance (Csp) can be calculated by fallowing equation:

$$\mathrm{C}s = \frac{I\Delta t}{m\Delta V} \text{ (F/g)}$$

Where 'I' is the applied current, Δt is the discharge time (or charge time), m is an active mass of catalyst or sample and 'ΔV' is the potential window under which experiment were performed.